Developmental Biology **247,** 197–209 (2002)
doi:10.1006/dbio.2002.0689

Formation of the Carotid Body in the Mouse Embryos

Yoko Kameda,*,[1] Toshiyuki Nishimaki,* Masatoshi Takeichi,† and Osamu Chisaka†

**Department of Anatomy, Kitasato University School of Medicine, Sagamihara, Kanagawa 228-8555, Japan; and †Department of Cell and Developmental Biology, Graduate School of Biostudies, Kyoto University, Sakyo-ku, Kyoto 606-8502, Japan*

Homeobox gene *Hoxa3* is strongly expressed in the third pharyngeal arch and pouch. We found that *Hoxa3* homozygous null mutant mice had the lack of the carotid body. In all late-term mutant embryos examined ($n = 10$), no carotid body was present. The carotid body rudiment is formed in the wall of the third branchial artery, which develops into the common carotid artery and the first part of the internal carotid artery. The symmetrical patterns of the third, fourth, and sixth arch arteries were observed in wild-type littermates at embryonic day (E) 10.5–12.5. In *Hoxa3* homozygous mutant embryos, however, the third arch artery began to degenerate at E10.5 and almost disappeared at E11.5. Furthermore, the bifurcation of the common carotid artery at the normal position, i.e., at the upper end of the larynx, was never detected in the mutant embryos at E16.5–E18.5. The common carotid artery of the homozygous mutants was separated into the internal and external carotid arteries immediately after its origin. Thus, the present study evidenced that the absence of the carotid body in *Hoxa3* homozygous mutants is due to the defect of development of the third arch artery, resulting in malformation of the carotid artery system. During fetal development, the carotid body of mice is in close association with the superior cervical ganglion of the sympathetic trunk. The superior cervical ganglion rather showed hypertrophic features in *Hoxa3* homozygous mutants lacking the carotid body.

***Key Words:* *Hoxa3* gene; carotid body; knockout mice; third arch artery; superior cervical ganglion of the sympathetic trunk; carotid artery.**

INTRODUCTION

The carotid body is a chemosensory organ which reacts sensitively to hypoxia, hypercapnia, and acidic pH in blood. The organ of mammalian species is situated in the carotid artery bifurcation and in close proximity to the superior cervical ganglion of the sympathetic trunk (Clarke and de Burgh Daly, 1981). It is innervated by the carotid sinus nerve issuing from the glossopharyngeal nerve and also by the ganglioglomerular nerve from the superior cervical ganglion (Verna, 1979). The chemosensory impulse which is conveyed by the carotid sinus nerve from the carotid body to the brain stem plays an important role in the reflex control of respiration and circulation (Gonzalez *et al.*, 1994). The carotid body consists mainly of two types of cells, i.e., glomus cell (chief or type I cell) and sustentacular cell (type II cell). Various types of neuroactive agents are contained in the glomus cells: biogenic amines, including serotonin, dopamine, and noradrenaline; catecholamine-synthesizing enzymes; and neuropeptides, including enkephalin and neuropeptide Y (Chiocchio *et al.*, 1966; Lundberg *et al.*, 1979; Kameda, 1990a; Oomori *et al.*, 1994). These substances are thought to modulate chemosensory activity by acting on afferent nerve terminals. The sustentacular cells exhibit immunoreactivity for vimentin, which is an intermediate-sized filament expressed in mesenchymal cells and glia-lineage cells (Kameda, 1996).

It is known in mammalian species that an accumulation of cells around the third branchial artery represents the first morphological sign of the carotid body development (Kondo, 1975). The cells from the sympathetic trunk have

[1] To whom correspondence should be addressed. Fax: +81-42-778-8441. E-mail: kameda@med.kitasato-u.ac.jp.

0012-1606/02 $35.00

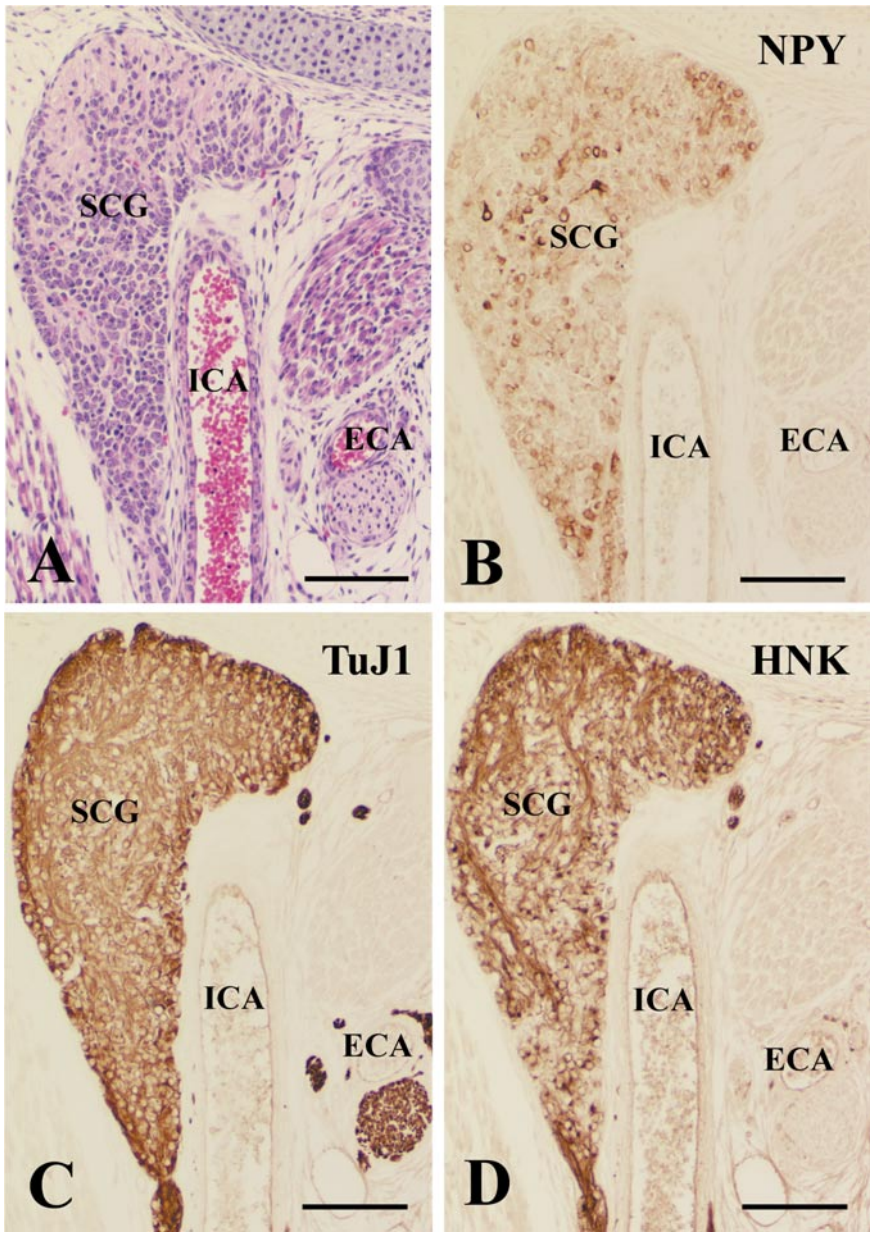

FIG. 1. Consecutive frontal sections showing the lack of the carotid body in the *Hoxa3* homozygous mutant mouse at E18.5. Hematoxylin–eosin staining (A). Immunostaining for neuropeptide Y (NPY) (B), TuJ1 (C), and HNK-1 (D) by the streptavidin–biotin–peroxidase method. In the superior cervical ganglion (SCG) of the sympathetic trunk, there is no cell stream running toward the carotid artery. ECA, external carotid artery; ICA, internal carotid artery. Scale bar, 100 μm.

been reported to continue with the carotid body primordium in human fetuses (Korkala and Hervonen, 1973). Using the quail-chick chimeras, the carotid body primordium has been shown to be colonized by cells derived from the neural crest (Le Douarin *et al.*, 1972). In contrast to mammalian species, in the chicken, the carotid body, together with the ultimobranchial gland, is located close to the distal (nodose) ganglion of the vagus nerve at the origin of the common carotid artery, i.e., being in the cervicothoracic border (Kameda *et al.*, 1988). It has been demonstrated by electron microscopy and immunohistochemistry that, in chick embryos, the carotid body rudiment formed in the wall of the third arch artery is composed of mesenchymal cells, whereas the cells immunoreactive for TuJ1, PGP 9.5, and HNK-1, all of which are markers for neurons, continuing with the distal vagal ganglion, initially surround and

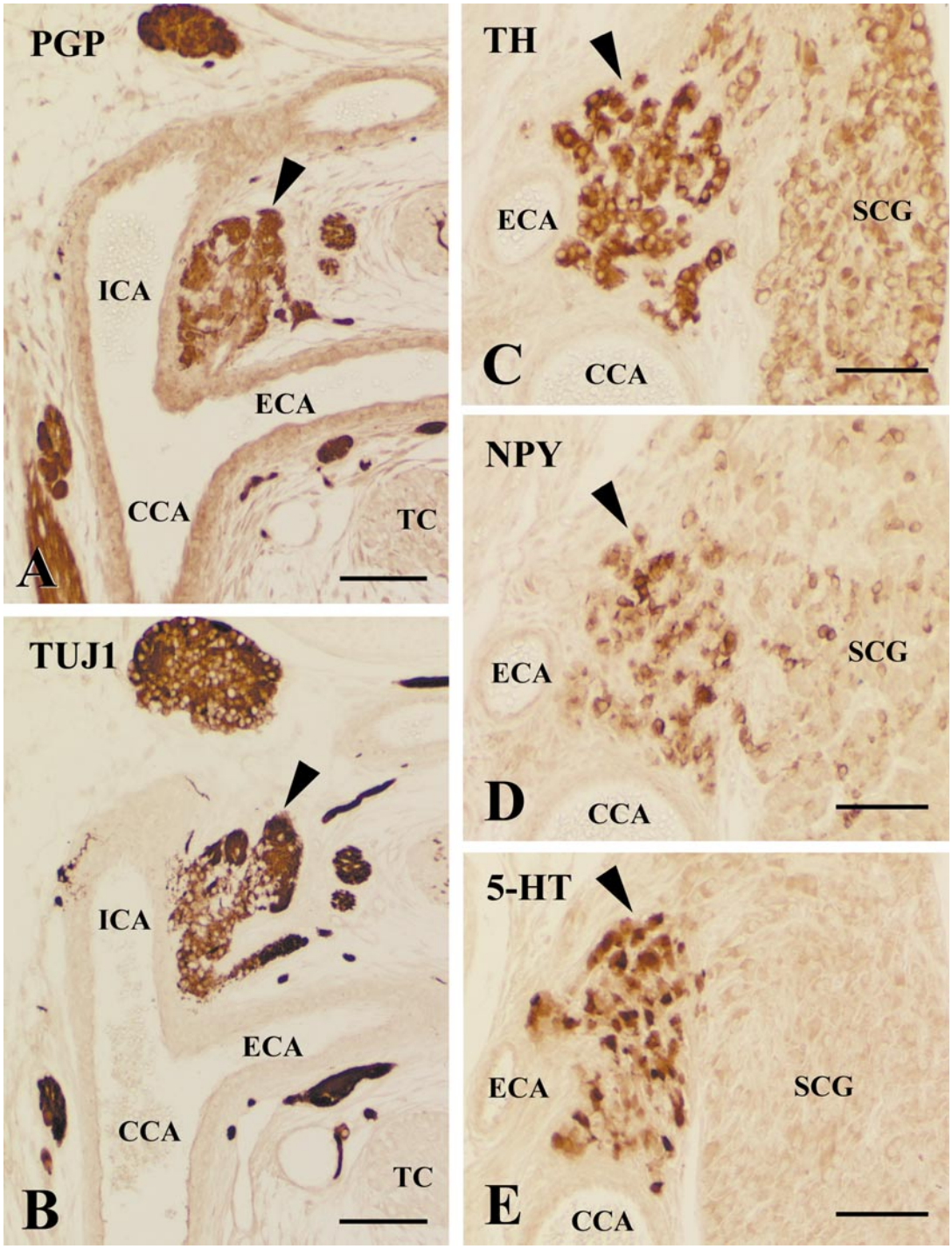

FIG. 2. (A, B) Consecutive sagittal sections of the carotid body (arrowhead) in a wild-type mouse at E16.5, stained by the streptavidin–biotin–peroxidase method with the PGP 9.5 (A) or TuJ1 antibody (B). Glomus cells express immunoreactivity for PGP 9.5 and TuJ1. (C–E) Consecutive frontal sections of the carotid body (arrowhead) and the superior cervical ganglion (SCG) in a wild-type mouse at E18.5, stained with different antisera. Glomus cells are immunoreactive for tyrosine hydroxylase (TH) (C), neuropeptide Y (NPY) (D), and serotonin (5-HT) (E). CCA, common carotid artery; ECA, external carotid artery; ICA, internal carotid artery; TC, thyroid cartilage. Scale bars, 80 μm in (A, B), and 60 μm in (C–E).

then invade the rudiment to become glomus cells (Kameda, 1994; Kameda *et al.*, 1994). Thus, the carotid body may be constituted either by mesenchymal cells forming the wall of the third arch artery or by neural cells continuous with the neighboring ganglion in the bird. Little information, however, is available concerning the immunohistochemical development of the carotid body in mammalian species.

In vertebrates, there are 39 *Hox* genes with some structural homology approximately 120 kb in length, which are organized in four different chromosomal complexes (see Krumlauf, 1994 for review). *Hox* genes encode a class of transcription factors that are used to orchestrate the morphological regionalization of embryos along its major axes. Our previous study has demonstrated that *Hoxa3* homozygous null mutant mice, made by gene targeting, are characterized by a spectrum of abnormalities, including the absence of thymus and parathyroid glands, reduced thyroid gland, a range of cardiovascular defects, and poorly developed throat cartilage (Chisaka and Capecchi, 1991). Thus, *Hoxa3* homozygous mutants mainly exhibit malformation of organs arising from the third and fourth pharyngeal arches and pouches. It has been shown by the quail-chick chimera system that most of the mesenchyme of the pharyngeal arches and pouches, including the mesenchyme of the thymus, parathyroid, and thyroid glands, and the outer walls of the blood vessels are derived from neural crest cells that migrate from the hindbrain neural folds (Le Lièvre and Le Douarin, 1975; Le Douarin, 1982). The connective tissue derivatives of neural crest seem to participate in the patterning of the pharyngeal arches and their derivatives, including the aortic arch arteries (Kirby and Waldo, 1995).

Since the carotid body rudiment is formed in the wall of the third arch artery, its formation may depend on the *Hoxa3* gene. However, the molecular mechanisms that determine the carotid body development remain unclear. To clarify the function of *Hoxa3* in organogenesis of the carotid body, we have analyzed embryonic mice bearing a *Hoxa3* homozygous null mutation, in comparison with the littermate wild types. Furthermore, this study defines by immunohistochemical study when and where the carotid body rudiment develops in the mouse embryos and how its formation is related to the *Hoxa3* gene.

MATERIALS AND METHODS

Hoxa3 Null Mutant Mouse

Targeted disruption of the *Hoxa3* gene, production of chimeric mice, and determination of genotype by polymerase chain reaction have been reported previously (Chisaka and Capecchi, 1991; Watari *et al.*, 2001). Noon on the day of which a copulation plug was found was designated as embryonic day 0.5 (E0.5).

Embryos were collected for analysis between E10.5 and E18.5. For histological study, the specimens were fixed in Bouin's solution for 24–48 h, embedded in paraffin, and then serially sectioned in the cross, frontal, or sagittal plane at a thickness of 5 μm. Selective sections were stained with hematoxylin–eosin to help determine morphological orientation.

Immunohistochemistry

Immunohistochemical staining was carried out by the streptavidin–biotin–peroxidase method as described previously (Kameda *et al.*, 1994). The following primary antibodies were employed: the monoclonal antibody TuJ1 to the neuron-specific class III β-tubulin isotype, the monoclonal antibody HNK-1 (Leu-7) to human lymphocyte antigen, the monoclonal antibody to α-smooth muscle actin, the polyclonal anti-human protein gene product (PGP) 9.5, anti-serotonin (5-HT), anti-neuropeptide Y, and anti-tyrosine hydroxylase antisera. The TuJ1 antibody was purchased from Berkeley antibody company (Richmond, CA) and used at a dilution of 1:500. The HNK-1 antibody was purchased from Becton Dickinson (San Jose, CA) and used at a dilution of 1:10. The diluted α-smooth muscle actin antibody was purchased from Dako (Carpinteria, CA). The PGP 9.5 antiserum was purchased from UltraClone Limited (Isle of Wight, UK) and used at a dilution of 1:600. The anti-5-HT antiserum was purchased from Chemicon (El Segundo, CA), anti-neuropeptide Y antiserum was purchased from UCB Bioproducts (Brussels, Belgium), and anti-bovine adrenal tyrosine hydroxylase antiserum was purchased from Eugene Tech International (Court Alendale, NJ). They were used at dilutions of 1:1000–1:2000.

Ink Injections

For the injection of India ink, embryos were collected at E11.5–E12.5, and undiluted ink was injected into the left ventricle by using a finely drawn glass pipette. The embryos were immediately fixed in 4% paraformaldehyde in phosphate buffer overnight. They were then dehydrated and immersed in a 50:50 mixture of benzyl benzoate and benzyl alcohol, until the body was cleared. In E18.5 animals, 10% red carbon ink in 10% gelatin solution was injected to clarify the carotid artery.

Quantitative Analysis

To compare the size of the superior cervical ganglion of the sympathetic trunk in the wild-type, heterozygous, and homozygous mutant embryos, the largest profile area of the ganglion on each side at E16.5 was photographed. Images of photographed ganglions were digitized by using a digital camera system (Fujix HC-2500; Fuji Film, Tokyo) attached to an Olympus AX80 microscope. Morphometric quantification was performed by using MacScope Image software (version 2.59; Mitani Corp., Fukui, Japan) on a Macintosh computer. The outline of the superior cervical ganglion was traced by hand and the profile area was assessed automatically by color binarization.

RESULTS

Carotid Body in Hoxa3 Homozygous Mutants and Wild-Type Littermates

As the homozygous null mutants of the *Hoxa3* gene die at or shortly after birth, the late-term embryos were examined. In all *Hoxa3* homozygous mutants examined ($n = 5$ for 18.5-day-old embryos; $n = 1$ for 17.5-day-old embryos;

n = 4 for 16.5-day-old embryos), no carotid body was detected (Figs. 1A–1D).

In wild-type littermates of 16.5- to 18.5-day-old embryos, the carotid body was detected in the region of the carotid bifurcation (Figs. 2A and 2B). At these stages of development, immunoreactivity for TuJ1 and PGP 9.5, which are specific markers for neurons, were expressed in the glomus cells of the carotid body. The carotid body always continued with the superior cervical ganglion of the sympathetic trunk during embryonic development. The connection between the carotid body and the ganglion was clarified in the frontal sections (Figs. 2C–2E and 3A–3D). The perikarya of neurons in the superior cervical ganglion were immunoreactive for tyrosine hydroxylase, the rate-limiting enzyme for catecholamine synthesis, and neuropeptide Y. Not only the neurons of the superior cervical ganglion, but also the glomus cells displayed immunoreactivity for tyrosine hydroxylase and neuropeptide Y (Figs. 2C and 2D). The immunoreactivity for tyrosine hydroxylase and neuropeptide Y was more intense in the glomus cells than the superior cervical ganglion. The glomus cells also exhibited immunoreactivity for 5-HT, whereas no immunoreactivity for 5-HT was detected in the superior cervical ganglion (Fig. 2E).

Nerve fibers immunoreactive for TuJ1 and PGP 9.5 were distributed within the carotid body parenchyma. The carotid sinus nerve derived from the glossopharyngeal nerve and the ganglioglomerular nerve derived from the superior cervical ganglion may contribute mainly to innervation of the carotid body. There were streams of both nerve fascicles and perikarya of neurons from the superior cervical ganglion to the carotid body (Fig. 3A). Neurons in the superior cervical ganglion were intensely immunoreactive for HNK-1, PGP 9.5, and TuJ1 (Figs. 3B–3D). Since the glomus cells were immunoreactive for TuJ1 and PGP 9.5, clear distinction of both organs, i.e., the carotid body and the superior cervical ganglion, was difficult in the sections stained with TuJ1 and PGP 9.5 antibodies. Unlike TuJ1 and PGP 9.5 antibodies, HNK-1 antibody hardly reacted with glomus cells (Fig. 3B). Thick nerve bundles immunoreactive for HNK-1 arising from the superior cervical ganglion penetrated the carotid body parenchyma

The Superior Cervical Ganglion of Sympathetic Trunk in Hoxa3 Homozygous Mutants

Hoxa3 homozygous mutant embryos have no carotid body. To clarify whether or not the lack of the carotid body in the homozygotes is due to the defective contribution of the superior cervical ganglion, the largest profile area of the ganglion was estimated in the frontal or sagittal sections of 16.5-day-old embryos (Table 1). The size of the superior cervical ganglion was rather increased in null mutants. In addition, it was confirmed in the frontal sections that, unlike wild types, there were no cell streams in the superior cervical ganglion, which run toward the carotid artery, in homozygous mutants (Figs. 1A–1D).

TABLE 1
The Size of the SCG of the Sympathetic Trunk at E16.5

Genotype	Sample number	Profile area of SCG (mm^2)
+/+	9	0.113 ± 0.007
+/−	5	0.141 ± 0.006*
−/−	8	0.162 ± 0.012**

Note. +/+, +/−, and −/− are wild-type, heterozygous, and homozygous mutants, respectively. Values are means ± SE.
*, $P < 0.05$; **, $P < 0.01$ vs wild types assessed by Student's t test.

The Carotid Artery in Hoxa3 Homozygous Mutants

The carotid artery system was abnormal in *Hoxa3* homozygous mutants. The origins of the internal and external carotid arteries were examined after intracardiac injection of red carbon ink/gelatin solution at E18.5. In wild-type littermates, the common carotid artery bifurcates into the internal and external carotid arteries at the upper end of the larynx (Fig. 4A). In the homozygous mutant mice, however, the carotid bifurcation was never detected at that level. The internal and external carotid arteries were separated at lower positions (Fig. 4B). In all homozygous mutants (n = 6), the common carotid artery bifurcated immediately after its origin, or the external or internal carotid arteries arose independently and there was therefore no common carotid artery.

The defect of the common carotid artery in *Hoxa3* homozygous mutants was also confirmed in both the sagittal and frontal sections. There was no carotid bifurcation at the upper end of the larynx, i.e., at the level of the thyroid cartilage, in the homozygotes (Fig. 4C; compare with Figs. 2A and 2B in wild type). Both the internal and the external carotid arteries arose directly from the brachiocephalic trunk at the right side, as shown in Fig. 4D. Thus, the defect of the carotid bifurcation at the normal position may be a significant factor inducing a lack of the carotid body.

Formation and Development of the Carotid Body

To determine the etiology of these late-term defects, the morphogenesis of the carotid body was studied throughout development. At E13.0, the carotid body rudiment first appeared as aggregations of cells in the medial wall of the third branchial artery (the common carotid artery and the origin of the internal carotid artery) in wild types (Figs. 5A and 5B). Some neural cells immunoreactive for PGP 9.5, which were continuous with the superior cervical ganglion, were encountered around the rudiment. The external carotid artery was identified near the third branchial artery at this stage. At E13.5, the carotid body rudiment became prominent and was located in the ventromedial wall of the origin of the internal carotid artery, being situated between the internal and the external carotid arteries (Figs. 5C and

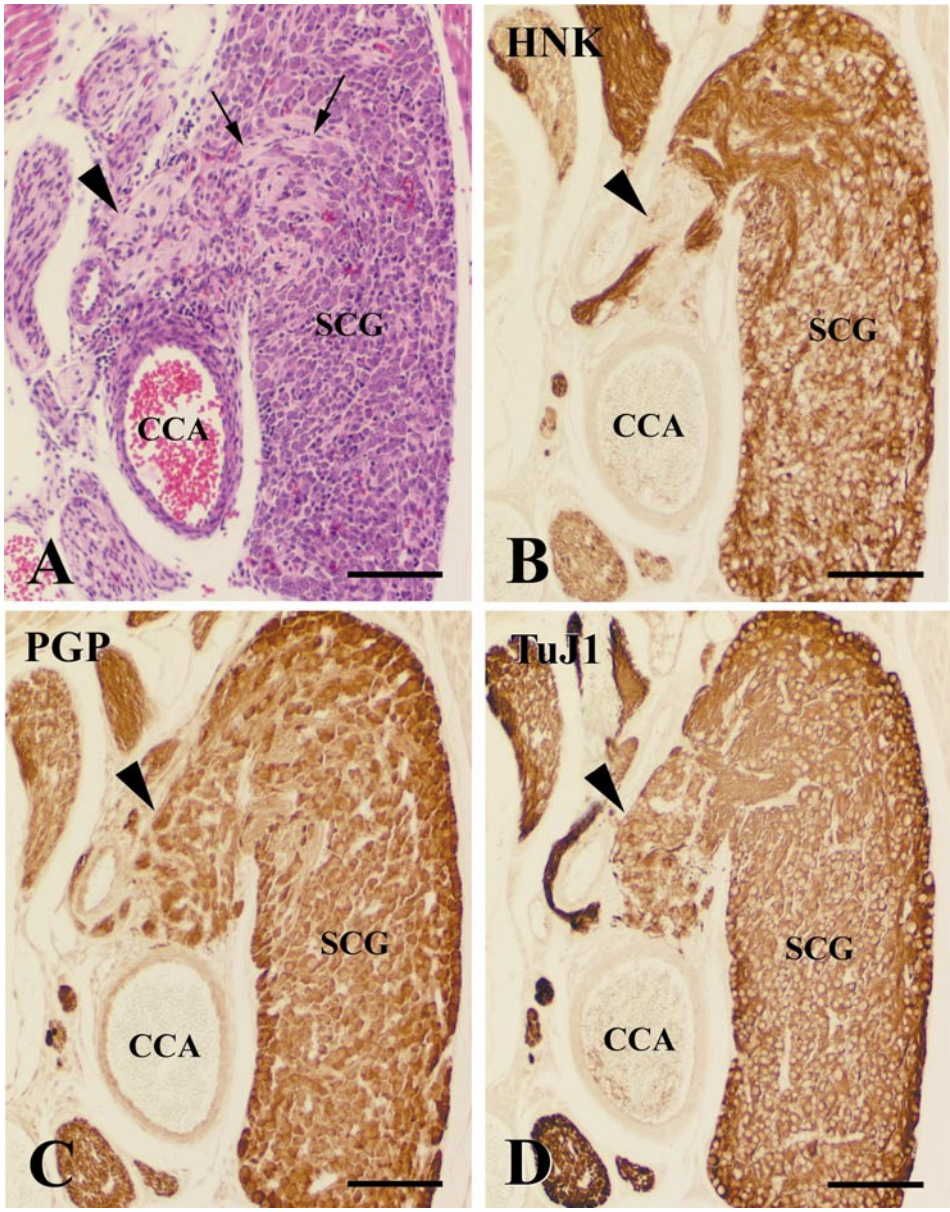

FIG. 3. Consecutive frontal sections showing the relationship between the carotid body (arrowhead) and the superior cervical ganglion (SCG) in a wild-type mouse at E18.5. Hematoxyin–eosin staining (A). The carotid body is adjacent to the upper end of the common carotid artery (CCA). Streams (arrows) of nerve fascicles from the superior cervical ganglion to the carotid body are observed. Immunostaining for HNK-1 (B), PGP 9.5 (C), and TuJ1 (D). Neurons in the superior cervical ganglion display immunoreactivity for HNK-1, PGP 9.5, and TuJ1. Glomus cells of the carotid body are also immunoreactive for PGP 9.5 and TuJ1, but show no immunoreactivity for HNK-1. Scale bar, 100 μm.

FIG. 4. (A, B) Comparison of the carotid artery system in *Hoxa3* wild-type (+/+, A) and homozygous mutant mice (−/−, B) at E18.5. Arteries were filled with red carbon ink. Left auricle (LA) was partially removed to facilitate visualization of the pulmonary trunk (PT). Arrowheads indicate the carotid artery bifurcation in a wild type. The common carotid artery (CCA) is very short in the mutant. In particular, the right common carotid artery (RCCA) is defective and the external carotid artery (ECA) and internal carotid artery (ICA) arise immediately from the brachiocephalic trunk (BCT). (C, D) Sagittal sections of the carotid arteries in the homozygous mutants at E18.5 (C) and E14.5 (D). Hematoxylin–eosin staining. The carotid bifurcation is not seen at the normal position (C). The internal and external carotid arteries are bifurcated just above the brachiocephalic trunk at the right side (D). AA, aortic arch; LCCA, left common carotid artery; LSCA, left subclavian artery; PT, pulmonary trunk; RA, right auricle; RSCA, right subclavian artery; SCG, superior cervical ganglion; TC, thyroid cartilage. Scale bars, 900 μm in (A, B), 100 μm in (C), and 80 μm in (D).

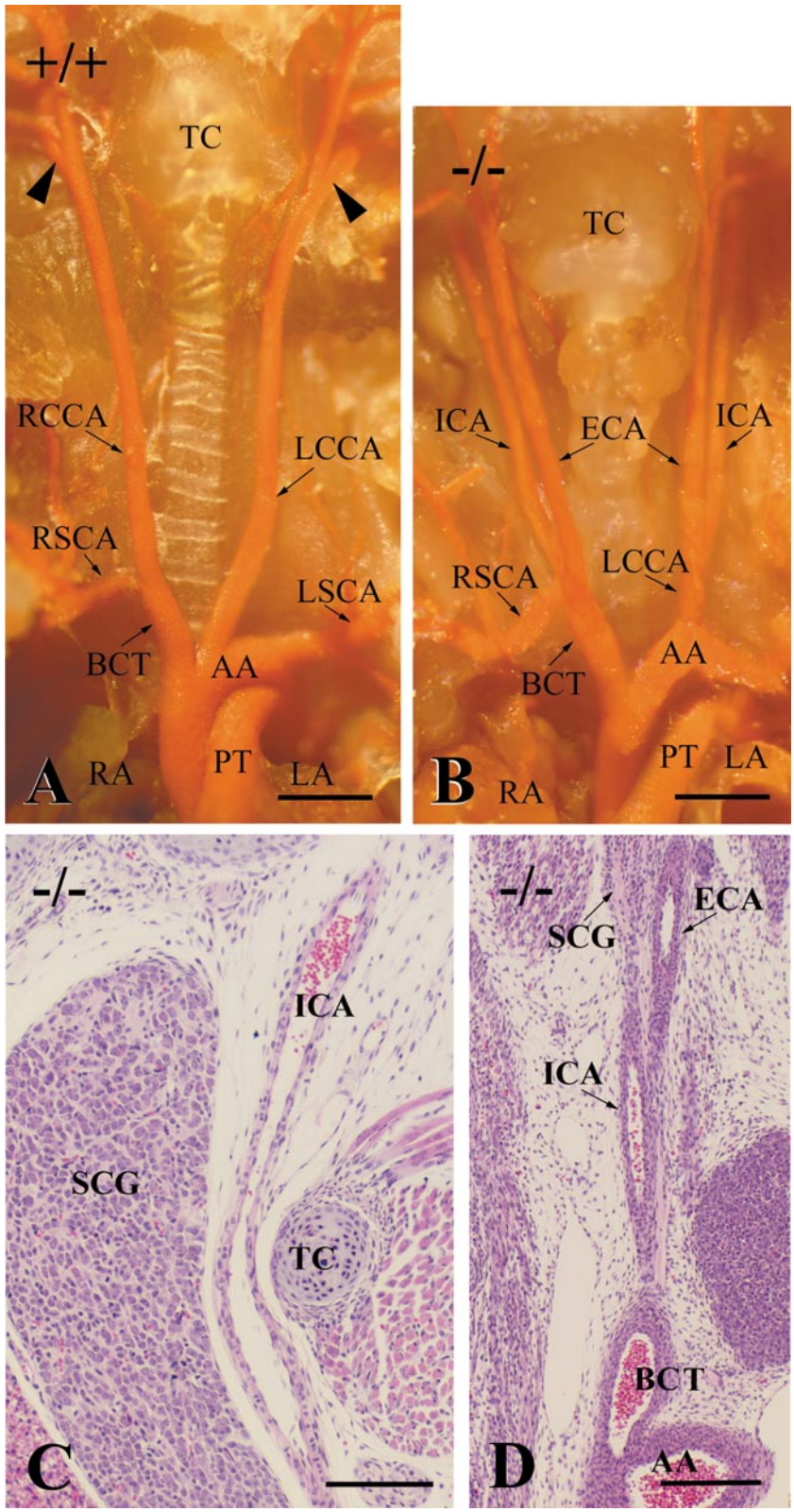

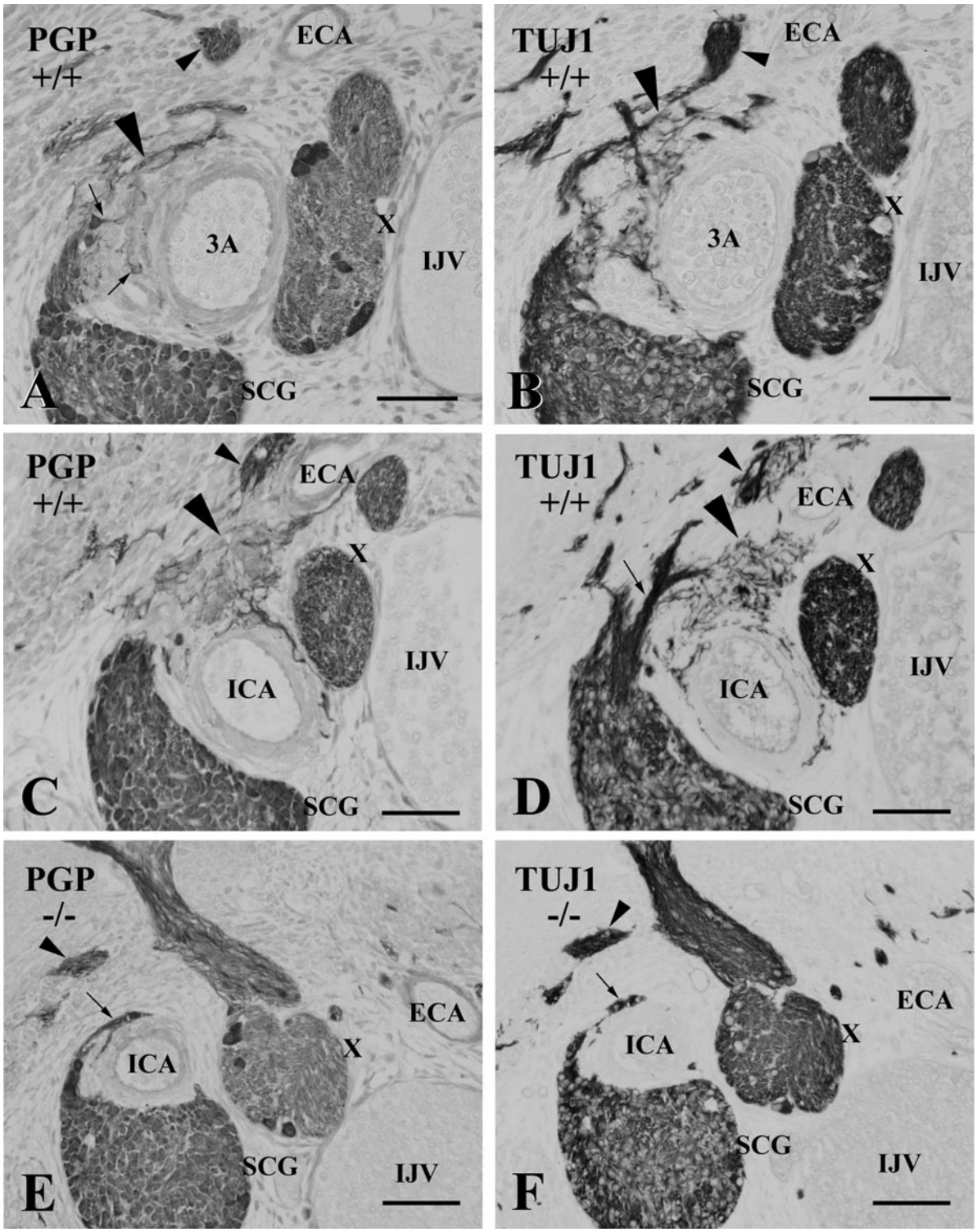

FIG. 5. (A, B) Consecutive transverse sections of the carotid body rudiment (large arrowhead) in wild type (+/+) at E13.0, stained with the PGP 9.5 (A) or TuJ1 antibody (B). PGP 9.5-immunoreactive cells (arrows) continuous with the superior cervical ganglion (SCG) surround the rudiment. Dense plexuses of TuJ1-immunoreactive fibers issuing from both the superior cervical ganglion and the glossopharyngeal nerve (small arrowhead) are distributed within the carotid body. (C, D) Consecutive transverse sections of the carotid body rudiment (large arrowhead) in wild type (+/+) at E13.5, stained with the PGP 9.5 (C) or TuJ1 antibody (D). At this stage, glomus cells in the carotid body rudiment show faint immunoreactivity for PGP 9.5 and TuJ1. Arrow indicates the nerve fascicles which originate from the superior cervical ganglion and enter the carotid body rudiment. Small arrowhead

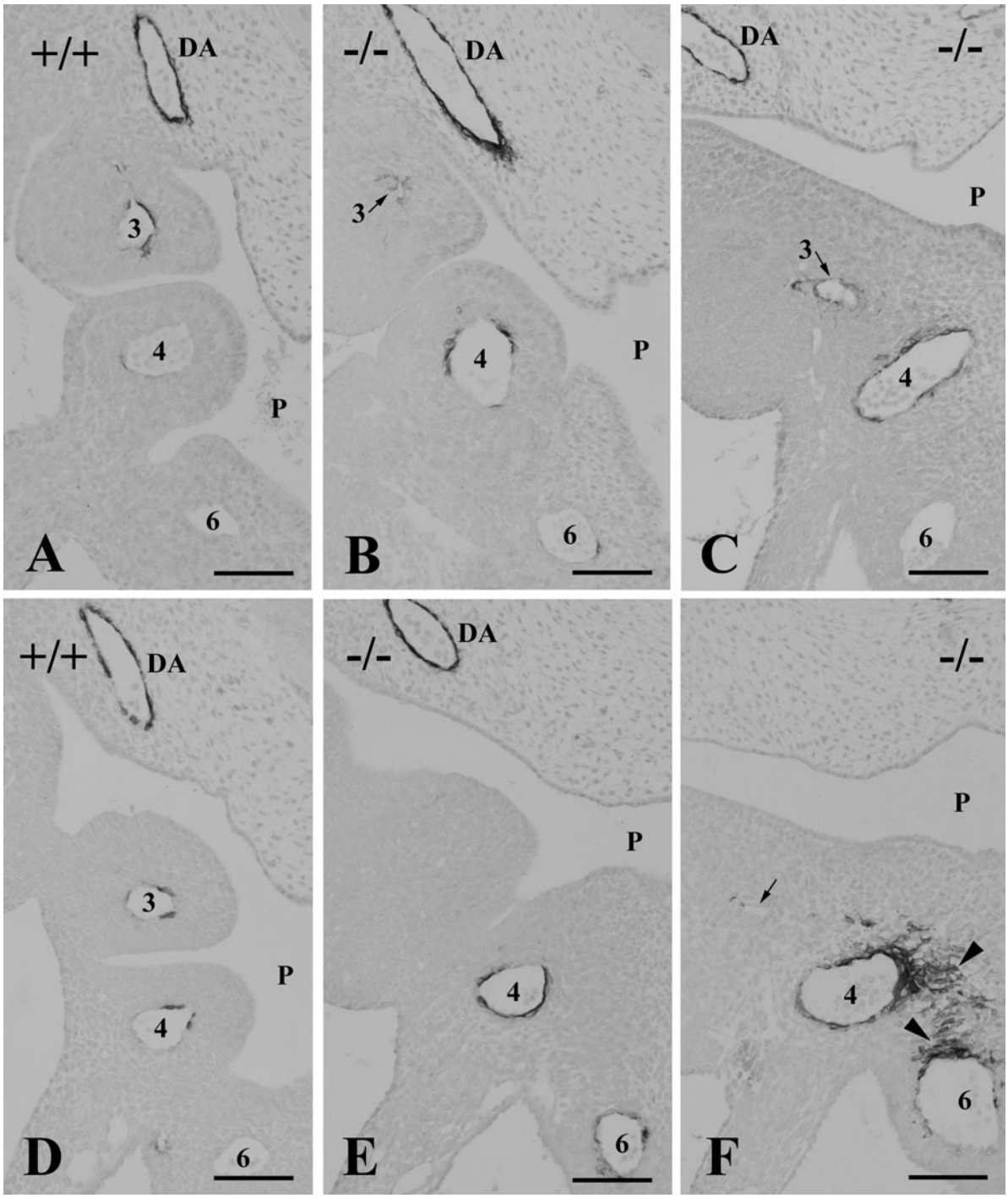

FIG. 6. The third (3), fourth (4), and sixth (6) arch arteries in *Hoxa3* wild types (+/+, A and D) and homozygous mutants (−/−, B, C, E, F), stained with α-smooth muscle actin antibody. At E10.5 (A–C), the third arch artery immunoreactive for α-actin is detected in serial sections of a homozygous mutant (B, C) as well as a wild type (A). At E11.5 (D–F), the third arch artery almost disappears in a homozygous mouse (E, F), in contrast to a wild type (D). Arrow indicates the vestige of the third arch artery. The fourth and sixth arch arteries are well developed in the homozygote and show accumulations of immunoreactive cells (arrowheads). DA, dorsal aorta; P, pharynx. Scale bar, 80 μm.

shows glossopharyngeal nerve. (E, F) Consecutive transverse sections showing the lack of the carotid body in a *Hoxa3* homozygous mutant (−/−) at E13.5, stained with the PGP 9.5 (E) or TuJ1 antibody (F). No carotid body is present close to the internal carotid artery (ICA), although the artery is surrounded by nerve fascicules and neurons (arrow) derived from the superior cervical ganglion. 3A, third arch artery; ECA, external carotid artery; ICA, internal carotid artery; IJV, internal jugular vein; SCG, superior cervical ganglion; X, vagus nerve. Scale bar, 60 μm.

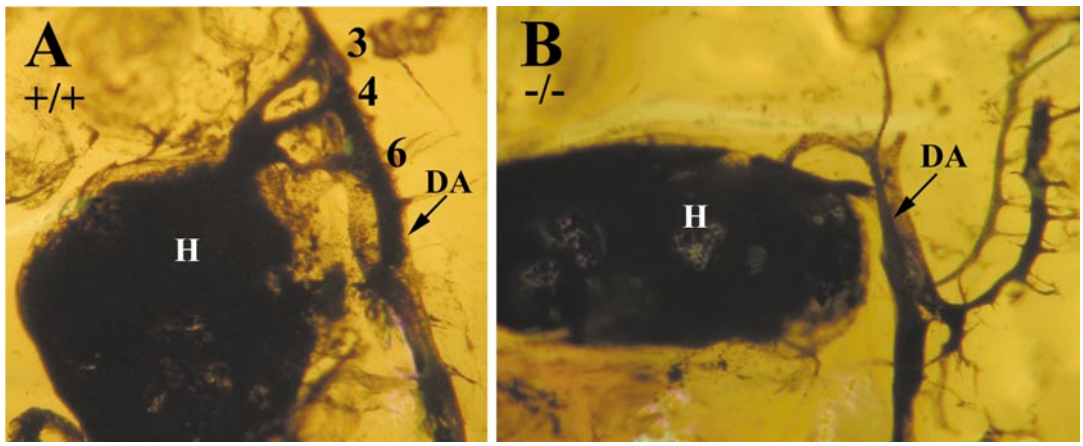

FIG. 7. Intracardiac ink injections at E12.5. Wild-type (+/+) embryo shows the formation of the third (3), fourth (4), and sixth (6) arch arteries (A). On the other hand, the *Hoxa3* homozygous mutant (−/−) has a lack of the third arch artery (B). DA, dorsal aorta; H, heart.

5D). The medial or ventromedial wall of the internal carotid artery showing the expansion for the carotid body rudiment was always surrounded by nerve fascicles and neural cells derived from the superior cervical ganglion at E13.0 and E13.5 (Figs. 5A–5D). Furthermore, nerve fascicles, which probably arise from the glossopharyngeal nerve, ran ventrally close to the carotid body rudiment. Dense plexuses of nerve fibers immunoreactive for TuJ1 were distributed within the carotid body rudiment (Figs. 5B and 5D). At E13.5, the immunoreactivity for PGP 9.5 and TuJ1 began to appear faintly in the glomus cells of the carotid body (Figs. 5C and 5D). At E14.5, the cells in the carotid body were intensely immunoreactive for both PGP 9.5 and TuJ1, and the connection between the carotid body and the superior cervical ganglion became distinct (data not shown).

Hoxa3 Homozygous Mutants at Early Stages of Development

In all *Hoxa3* homozygous mutants examined in cross-sections ($n = 3$ for 13.0-day-old embryos; $n = 4$ for 13.5-day-old embryos), no cell aggregation, i.e., the carotid body rudiment, was formed in the wall of the third branchial (internal carotid) artery (Figs. 5E and 5F). The artery of homozygous mutants, as well as wild types, was surrounded by the nerve fascicles and neuronal cells originating from the superior cervical ganglion (Figs. 5E and 5F). The external carotid artery was detected separate from the internal carotid artery in the homozygous mutants (Figs. 5E and 5F). Furthermore, diameter and profile area of the internal carotid artery were small compared with those in wild types.

Pharyngeal Arch Arteries

The development of the arch arteries was examined by immunohistochemistry with the monoclonal antibody to α-smooth muscle actin. The third, fourth, and sixth arch arteries were centrally localized in their pharyngeal arches, respectively, in wild types at E10.5 and E11.5 (Figs. 6A and 6D). Immunoreactivity for α-actin was detected in the wall of the third arch artery in addition to the dorsal aorta at E10.5 (Fig. 6A). In *Hoxa3* null mutants, the third arch artery was in the process of degeneration at E10.5 (Fig. 6B). Immunoreactivity for α-actin, however, was clearly detected in the wall of the third arch artery, particularly at the ventral part (Fig. 6C). The fourth arch artery of the homozygous embryos exhibited more intense immunoreactivity for α-actin and larger diameter than that of wild types. At E11.5, the third arch artery in the homozygous mutants almost disappeared and displayed little α-actin immunoreactivity, whereas the fourth and sixth arch arteries were more developed. In particular, accumulations of α-actin immunoreactive cells were identified around the fourth and sixth arch arteries near the aortic sac in the mutant embryos (Fig. 6F). The size and amount of mesenchyme of the third pharyngeal arch in the mutants were similar to those in the wild types.

To investigate the development of arch arteries, the intracardiac injection of India ink was carried out in *Hoxa3* homozygous mutants and wild types at E11.5–E12.5. In wild-type embryos, the third, fourth, and sixth arch arteries were detected in a bilaterally symmetrical pattern and connected with the left or right dorsal aorta (Fig. 7A). In contrast, in all *Hoxa3* null mutant embryos examined ($n = 8$ from 5 dams), the third arch artery was absent (Fig. 7B).

DISCUSSION

Hoxa3 plays a crucial role for formation of the third pharyngeal arch and pouch (Chisaka and Capecchi, 1991). The carotid body rudiment is formed in the wall of the third arch artery (Kondo, 1975; Kameda *et al.*, 1994). We found

that null mutation of *Hoxa3* resulted in a defect in formation of the carotid body. There was no carotid body in all homozygous mutant mice examined ($n = 10$) at E16.5–E18.5. It has been shown in quail-chick chimeras that the wall of the third arch artery is made up of mesenchymal cells originating from the neural crest (Le Lièvre and Le Douarin, 1975). In chick embryos with neural crest ablation, the proportion of mesenchyme in pharyngeal arches is markedly reduced and the regular pattern of paired arch vessels is missing (Bockman *et al.*, 1989). In mouse embryos, as well as avian species, neural crest-derived mesenchymal cells surround the arch arteries from the time of their formation (Waldo *et al.*, 1999; Jiang *et al.*, 2000). In particular, the third pharyngeal arch is filled with the neural crest cells. The derivatives of the third, fourth, and sixth arch arteries retain a substantial contribution of the neural crest cells (Jiang *et al.*, 2000). Thus, it is thought that the carotid body rudiment is formed by neural crest-derived mesenchymal cells investing the third arch artery. *In situ* hybridization study indicates that the *Hoxa3* gene is seen in the mesenchyme throughout the third arch of normal mouse embryos at E10.5 (Manley and Capecchi, 1995).

The present study indicated that, in *Hoxa3* homozygous mutants, the third arch artery immunoreactive for α-smooth muscle actin was present at E10.5, but the artery disappeared at E11.5. The size and amount of mesenchyme of the third pharyngeal arch in the mutants did not differ from those in the wild types at E10.5 and E11.5. The absence of the third arch artery at E11.5–E12.5 was also confirmed in the mutants given intracardiac injection of India ink. It seems that, in *Hoxa3* homozygous mutants, neural crest-derived mesenchymal cells surround the third arch artery to form the arterial wall, but the artery degenerates, such as the first and second arch arteries in wild types. In fact, the extensive labeling of lacZ is seen in each pharyngeal arch, including the third one of *Hoxa3* homozygous mice crossed by connexin 43-lacZ transgenic mice in which neural crest cells are specifically marked (Chisaka and Kameda, unpublished data). The cause of degeneration of the third arch artery in *Hoxa3* null mutants remains to be elucidated.

Since the third arch artery disappears after E11.5, the organization of the carotid artery system derived from the third arch artery was unusual in the mutant mice. The common carotid artery was absent or very short. The artery cannot bifurcate into the internal and external carotid arteries at the normal position, i.e., at the upper end of larynx. The derivatives of the third arch artery may be replaced by the cranial part of the dorsal aorta, i.e., the upper part connected with the fourth arch artery, in the mutants. As the external carotid artery branches from the third arch artery in normal animals, the artery may also branch from the dorsal aorta in *Hoxa3* mutants. The present study evidenced that the lack of the carotid body in the *Hoxa3* mutants is caused by the defect of the third arch artery, resulting in malformation of the carotid artery system.

In wild-type mouse embryos, the carotid body rudiment was first formed in the medial wall of the third arch artery at E13.0. The rudiment was recognized as cell masses receiving numerous nerve fibers derived from the superior cervical ganglion of the sympathetic trunk and from the glossopharyngeal nerve. In addition, the rudiment was surrounded by neural cells continuous with the superior cervical ganglion. In the bird, neural cells continuous with the distal vagal ganglion first surround the carotid body rudiment. The cells exhibit immunoreactivity for PGP 9.5, TuJ1, and HNK-1, which are specific markers for neurons, and further for 5-HT, chromogranin A, and tyrosine hydroxylase, which are phenotypic markers for glomus cells (Kameda *et al.*, 1990, 1994). The cells immunoreactive for these neuroproteins and amines then enter into the carotid body parenchyma, becoming glomus cells. The neural cells from the distal vagal ganglion invade not only the carotid body rudiment but also other portions of the wall of the third arch artery. Glomus cells of chickens, therefore, are widely distributed in the wall of the common carotid artery and around four arteries arising as one trunk from the common carotid artery (Kameda, 1990b). Although the neural cell population surrounding the carotid body rudiment was small in mouse embryos as compared with that in chick embryos, the cells derived from the superior cervical ganglion may give rise to glomus cells. It is probable that the carotid body is formed by two elements: one is mesenchymal neural crest cells investing the third arch artery and the other is neural cells derived from the neighboring ganglion. The nerve fascicles and neural cells continuous with the superior cervical ganglion surrounded the internal carotid artery in *Hoxa3* mutant embryos as well as wild types. The neural precursor cells from the superior cervical ganglion, however, are unable to differentiate into the glomus cells in the homozygous mutants, since no carotid body rudiment is present. Electron microscopic studies have reported that, in rats and rabbits, undifferentiated cells within the carotid body rudiment differentiate into glomus cells (Kondo, 1975; Kariya *et al.*, 1990). It is postulated that, in mammalian species, in addition to the neural cells derived from the superior cervical ganglion, the neural crest-derived mesenchymal cells in the carotid body rudiment are able to differentiate into the glomus cells by stimulation of the glossopharyngeal and sympathetic nerve fibers.

Sympathetic neurons embryologically originate from the neural crest (Le Douarin, 1982). The carotid body glomus cells express phenotypic markers for the sympathetic nerves, such as catecholamines, tyrosine hydroxylase, and neuropeptide Y. In mouse embryos, the carotid body rudiment was always surrounded by nerve fascicles arising from the superior cervical ganglion of the sympathetic trunk. Furthermore, the carotid body was intimately connected with the superior cervical ganglion during fetal development. In *Hoxa3* homozygous mutant mice, the carotid body was absent, whereas the superior cervical ganglion was enlarged in volume compared with that in wild types.

Sympathetic ganglia derived from neuronal neural crest may be scarcely affected by the *Hoxa3* gene. Hypertrophy of the superior cervical ganglion in the mutant embryos seems to reflect the defect of its target organ. It is thought that the nerve fibers originating from the superior cervical ganglion stimulate the formation of the carotid body rudiment in the wall of the third arch artery, and also differentiation and development of the glomus cells.

In a wide variety of animal species, substance P- and calcitonin gene-related peptide (CGRP)-immunoreactive fibers are densely distributed in the carotid body and form synaptic contacts with glomus cells (Kondo and Yamamoto, 1988; Kummer and Habeck, 1991). These sensory nerve fibers innervating the mammalian carotid body mainly come from the petrosal ganglion of the glossopharyngeal nerve via the carotid sinus nerve (Kummer, 1988; Czyzyk-Krzeska *et al.*, 1991; Ichikawa *et al.*, 1993). In the glossopharyngeal nerve, neurons of the proximal (jugular) ganglion are derived from neural crest, those of the distal (petrosal) ganglion from placodes, and Schwann cells and satellite cells of both ganglia originate from neural crest (D'Amico-Martel and Noden, 1983). The truncation of the glossopharyngeal nerve and its fusion with the distal vagal ganglion occur in *Hoxa3* homozygous mutants at E10.5 (Manley and Capecchi, 1997). In *Hoxa3* null mutation, however, peripheral branches of the placode-derived neurons in the petrosal ganglion exhibit an essentially normal projection pattern (Watari *et al.*, 2001). The lack of the carotid body in the *Hoxa3* mutant homozygotes may not be due to malformation of the glossopharyngeal nerve. The superior cervical ganglion of the sympathetic trunk and the carotid sinus nerve of the glossopharyngeal nerve seem to develop normally and project axons toward their target, i.e., the carotid body, in the *Hoxa3* homozygous mutants. It is thought that the lack of formation of the carotid body rather affects the superior cervical ganglion and the carotid sinus nerve. Hypertrophy of the superior cervical ganglion occurred in *Hoxa3* mutants.

A wide range of abnormalities appeared in the *Hoxa3* homozygotes that are similar to the pathology of the human DiGeorge syndrome (Chisaka and Capecchi, 1991). DiGeorge syndrome is usually associated with deletions of human chromosome 22q11. The syndrome has been postulated to depend on disturbance of migration or differentiation of neural crest cells into the pharyngeal arches, pouches, and cardiac outflow tract (Scambler, 2000). Aside from the *Hoxa3* mutant homozygotes, dominant disorders known as DiGeorge syndrome have been demonstrated in homozygous mutant mice for *Tbx1*, which encodes a transcription factor of the T-box family, and for *Crkol*, which is mice homologue of the human *CRKL* mapped within the common deletion region for DiGeorge syndrome (Jerome and Papaioannou, 2001; Guris *et al.*, 2001). Concerning the pharyngeal arch arteries, it has been reported that only a single arch artery is formed in *Tbx1* mutants, whereas the formation of the third, fourth, and sixth arch arteries is normal in $Crkol^{-/-}$ embryos. These studies have ignored whether or not $Tbx1^{-/-}$ and $Crkol^{-/-}$ mice show the carotid body defects.

REFERENCES

Bockman, D., Redmond, M., and Kirby, M. L. (1989). Alteration of early vascular development after ablation of cranial neural crest. *Anat. Rec.* **225,** 209–217.

Chiocchio, S. R., Biscardi, A. M., and Tramezzani, J. H. (1966). Catecholamines in the carotid body of the cat. *Nature* **19,** 834–835.

Clarke, J. A., and de Burgh Daly, M. (1981). A comparative study of the distribution of carotid body type-I cells and periadventitial type-I cells in the carotid bifurcation regions of the rabbit, rat, guinea-pig and mouse. *Cell Tissue Res.* **220,** 753–772.

Chisaka, O., and Capecchi, M. R. (1991). Regionally restricted developmental defects resulting from targeted disruption of the mouse homeobox gene *hox-1.5*. *Nature* **350,** 473–479.

Czyzyk-Krzeska, M. F., Bayliss, D. A., Lawson, E. E., and Millhorn, D. E. (1991). Expression of messenger RNAs for peptides and tyrosine hydroxylase in primary sensory neurons that innervate arterial baroreceptors and chemoreceptors. *Neurosci. Lett.* **129,** 98–102.

D'Amico-Martel, A., and Noden, D. M. (1983). Contributions of placodal and neural crest cells to avian cranial peripheral ganglia. *Am. J. Anat.* **166,** 445–468.

Gonzalez, C., Almaraz, L., Obeso, A., and Rgual, R. (1994). Carotid body chemoreceptors: From natural stimuli to sensory discharges. *Physiol. Rev.* **74,** 829–898.

Guris, D. L., Fantes, J., Tara, D., Druker, B. J., and Imamoto, A. (2001). Mice lacking the homologue of the human 22q11.2 gene *CRKL* phenocopy neurocristopathies of DiGeorge syndrome. *Nat. Genet.* **27,** 293–298.

Ichikawa, H., Rabchevsky, A., and Helke, C. J. (1993). Presence and coexistence of putative neurotransmitters in carotid sinus baro- and chemoreceptor afferent neurons. *Brain Res.* **611,** 67–74.

Jerome, L. A., and Papaioannou, V. E. (2001). DiGeorge syndrome phenotype in mice mutant for the T-box gene, *Tbx1*. *Nat. Genet.* **27,** 286–291.

Jiang, X., Rowitch, D. H., Soriano, P., McMahon, A. P., and Sucov, H. M. (2000). Fate of the mammalian cardiac neural crest. *Development* **127,** 1607–1616.

Kameda, Y. (1990a). Innervation of the serotonin-immunoreactive cells distributed in the wall of the common carotid artery and its branches in the chicken. *J. Comp. Neurol.* **292,** 537–550.

Kameda, Y. (1990b). Distribution of serotonin-immunoreactive cells around arteries arising from the common carotid artery in the chicken. *Anat. Rec.* **227,** 87–96.

Kameda, Y. (1994). Electron microscopic study on the development of the carotid body and glomus cell groups distributed in the wall of the common carotid artery and its branches in the chicken. *J. Comp. Neurol.* **348,** 544–555.

Kameda, Y. (1996). Immunoelectron microscopic localization of vimentin in sustentacular cells of the carotid body and the adrenal medulla of guinea pigs. *J. Histochem. Cytochem.* **44,** 1439–1449.

Kameda, Y., Okamoto, K., Ito, M., and Tagawa, T. (1988). Innervation of the C cells of chicken ultimobranchial glands studied by immunohistochemistry, fluorescence microscopy, and electron microscopy. *Am. J. Anat.* **182,** 353–368.

Kameda, Y., Amano, T., and Tagawa, T. (1990). Distribution and ontogeny of chromogranin A and tyrosine hydroxylase in the carotid body and glomus cells located in the wall of the common carotid artery and its branches in the chicken. *Histochemistry* **94,** 609–616.

Kameda, Y., Yamatsu, Y., Kameya, T., and Frankfurter, A. (1994). Glomus cell differentiation in the carotid body region of chick embryos studied by neuron-specific class III β-tubulin isotype and Leu-7 monoclonal antibodies. *J. Comp. Neurol.* **348,** 531–543.

Kariya, I., Nakajima, T., and Ozawa, H. (1990). Ultrastructural study on cell differentiation of the rabbit carotid body. *Arch. Histol. Cytol.* **53,** 245–258.

Kirby, M. L., and Waldo K. L. (1995). Neural crest and cardiovascular patterning. *Circ. Res.* **77,** 211–215.

Kondo, H. (1975). A light and electron microscopic study on the embryonic development of the rat carotid body. *Am. J. Anat.* **144,** 275–294.

Kondo, H., and Yamamoto, M. (1988). Occurrence, ontogeny, ultrastructure and some plasticity of CGRP (calcitonin gene-related peptide)-immunoreactive nerves in the carotid body of rats. *Brain Res.* **473,** 283–293.

Korkala, O., and Hervonen, A. (1973). Origin and development of the catecholamine-storing cells of the human fetal carotid body. *Histochemie* **37,** 287–297.

Krumlauf, R. (1994). *Hox* genes in vertebrate development. *Cell* **78,** 191–201.

Kummer, W. (1988). Retrograde neuronal labelling and double-staining immunohistochemistry of tachykinin- and calcitonin gene-related peptide-immunoreactive pathways in the carotid sinus nerve of the guinea pig. *J. Auton. Nerv. Syst.* **23,** 131–141.

Kummer, W., and Habeck, J. (1991). Substance P- and calcitonin gene-related peptide-like immunoreactivities in the human carotid body studied at light and electron microscopical level. *Brain Res.* **554,** 286–292.

Le Douarin, N. (1982). "The Neural Crest." Cambridge Univ. Press, Cambridge.

Le Douarin, N., Le Lièvre, M. C., and Fontaine, J. (1972). Recherches expérimentales sur l'origine embryologique du corps carotidien chez les oiseaux. *C. R. Acad. Sci. Hebd. Seances Acad. Sci. D* **275,** 583–586.

Le Lièvre, C. S., and Le Douarin, N. M. (1975). Mesenchymal derivatives of the neural crest: Analysis of chimaeric quail and chick embryos. *J. Embryol. Exp. Morphol.* **34,** 125–154.

Lundberg, J. M., Hökfelt, T., Fahrenkrug, J., Nilsson, G., and Terenius, L. (1979). Peptides in the cat carotid body (glomus caroticum): VIP-, enkephalin-, and substance P-like immunoreactivity. *Acta Physiol. Scand.* **107,** 279–281.

Manley, N. R., and Capecchi, M. R. (1995). The role of *Hoxa-3* in mouse thymus and thyroid development. *Development* **121,** 1989–2003.

Manley, N. R., and Capecchi, M. R. (1997). *Hox* group 3 paralogous genes act synergistically in the formation of somitic and neural crest-derived structures. *Dev. Biol.* **192,** 274–288.

Oomori, Y., Nakaya, K., Tanaka, H., Inchi, H., Ishikawa, K., Satoh, Y., and Ono, K. (1994). Immunohistochemical and histochemical evidence for the presence of noradrenaline, serotonin and gamma-aminobutyric acid in chief cells of the mouse carotid body. *Cell Tissue Res.* **278,** 249–254.

Scambler, P. J. (2000). The 22q11 deletion syndromes. *Hum. Mol. Genet.* **9,** 2421–2426.

Verna, A. (1979). Ultrastructure of the carotid body in the mammals. *Int. Rev. Cytol.* **60,** 271–330.

Waldo, K. L., Lo, C. W., and Kirby, M. L. (1999). Connexin 43 expression reflects neural crest patterns during cardiovascular development. *Dev. Biol.* **208,** 307–323.

Watari, N., Kameda, Y., Takeichi, M., and Chisaka, O. (2001). *Hoxa3* regulates integration of glossopharyngeal nerve precursor cells. *Dev. Biol.* **240,** 15–31.

Received for publication November 29, 2001
Revised March 20, 2002
Accepted April 1, 2002
Published online May 31, 2002